

X-ray induced reduction of the crystal of high-molecular weight cytochrome *c* revealed by microspectrophotometry

Midori Sato,^a Naoki Shibata,^a Yukio Morimoto,^{ab} Yuki Takayama,^c Kiyoshi Ozawa,^c Hideo Akutsu,^c Yoshiki Higuchi^{ab*} and Noritake Yasuoka^{ab}

^aHimeji Institute of Technology, 3-2-1 Koto, Kamigori-cho, Ako-gun, Hyogo 678-1297, Japan, ^bRIKEN Harima Institute/Spring-8, 1-1-1 Koto, Mikazuki-cho, Sayo-gun, Hyogo 679-5148, Japan, and ^cInstitute for Protein Research, Osaka University, Yamadaoka, Suita 565-0871, Japan.
E-mail: hig@sci.himeji-tech.ac.jp

The crystal structures of high-molecular weight cytochrome *c* (HMC) from *Desulfovibrio vulgaris* Hildenborough in the transient and reduced states have been determined at 2.8 Å resolution. An absorption spectrum measured with microspectrophotometer indicated that about 86% of the hemes were reduced after 45 min irradiation of x-ray beam. Further exposure for 90 min did not significantly change the spectrum. These results suggest that HMC in crystalline state is easily reduced by illumination of x-ray beam from synchrotron radiation.

Keywords: high-molecular weight cytochrome *c*; microspectroscopic measurement; 16 heme proteins; transient state; x-ray crystal structure.

1. Introduction

Sulfate-reducing bacteria are unique microorganism which contain several kinds of *c*-type cytochromes. The crystal structures of many cytochrome molecules have been reported at atomic resolution. They are tetra-heme cytochrome *c*₃ (*M*_r 14,000) (Haser *et al.*, 1979; Pierrot *et al.*, 1982; Higuchi *et al.*, 1984; Morimoto *et al.*, 1991; Czjzek *et al.*, 1994; Matias *et al.*, 1996), mono-heme cytochrome *c*-553 (*M*_r 9,000) (Nakagawa *et al.*, 1990), tri-heme cytochrome *c*₇ (*M*_r 8,500) (Czjzek *et al.*, 2001), nona-heme cytochrome *c* (9Hcc) (*M*_r 37,500) (Matias *et al.*, 1999; Fritz *et al.*, 2001), octa-heme cytochrome *c*₃ (*M*_r 26,000) (Czjzek *et al.*, 1996), and hexadeca-heme high-molecular weight cytochrome *c* (HMC) (*M*_r 66,000) (Czjzek *et al.*, 2002; Matias *et al.*, 2002). Cytochrome *c*-553 was reported to have a His-Met-coordinated heme, whereas tetra-heme cytochrome *c*₃, an electron carrier of hydrogenase, has four His-His-coordinated hemes in a single polypeptide chain.

HMC was discovered (Yagi, 1969) and characterized as a hexadeca-heme protein in a single polypeptide chain (Higuchi *et al.*, 1987). The elucidation of the physiological role of HMC has been one of the interesting subjects to understand the energy metabolism of the sulfate-reducing bacteria. HMC was reported to transfer electrons with [NiFe]hydrogenase through cytochrome *c*₃ at efficient rates (Matias *et al.*, 1999, 2002; Higuchi *et al.*, 1997). Since sulfate-reducing bacteria transfer electrons from the periplasm to cytoplasm, a transmembrane electron transfer system must be existed. The *hmc* operon from *Desulfovibrio vulgaris* Hildenborough was reported to be composed of six genes (Rossi *et al.*, 1993). Some of them encode transmembrane proteins, which form a redox complex with HMC. However, the electron pathway and the physiological role of this complex are still unknown.

Recent structural studies of 9Hcc from *Desulfovibrio desulfuricans* ATCC 27774 (Matias *et al.*, 1999) and *Desulfovibrio desulfuricans* Essex (Fritz *et al.*, 2001) and HMC from *Desulfovibrio vulgaris* Hildenborough (Czjzek *et al.*, 2002; Matias *et al.*, 2002) revealed that both of them are composed of a tetra-heme cytochrome *c*₃ motif as a basic component in their three dimensional structures. 9Hcc has two domains based on the location of the heme clusters, i.e. N-terminal five-heme (tetra-heme (Heme-1, 2, 3, and 5) and mono-heme (Heme-4)) domain, and C-terminal tetra-heme (Heme-6, 7, 8, and 9) domain. On the other hand, HMC has 4 domains, such as N-terminal tri-heme (Heme-1, 2, and 3), the second tetra-heme (Heme-4, 5, 6, and 7), the next 5 heme (tetra-heme (Heme-8, 9, 10, and 12) and mono-heme (Heme-11)), and C-terminal tetra-heme (Heme-13, 14, 15, and 16) domains. The spatial disposition of the heme groups and possible electron transfer pathways between tetra heme cytochrome *c*₃ was suggested from two crystal structures of HMC (Czjzek *et al.*, 2002; Matias *et al.*, 2002). In order to understand the mechanism of the electron transfer system, however, the detailed structural differences between the oxidized and reduced states must be presented with a sufficient accuracy. It was reported that x-ray beam from synchrotron radiation bring an unexpected effect to a heme protein, that is, substantial dose of x-ray beam caused the reduction of a heme group in peroxidase (Haser *et al.*, 2002). In this paper, we report the crystal structure of HMC from *D. vulgaris* Hildenborough at atomic resolution, and the effect of the reduction of hemes by illumination of x-ray beam from synchrotron radiation which was revealed by a visible absorption microspectrophotometry.

2. Material and method

2.1. Purification

The *hmc* gene from *Desulfovibrio vulgaris* Hildenborough was introduced into *shewanella oneidensis* using electroporation. Bacterial cells were obtained according to the method previously reported (Ozawa *et al.*, 2001). About 16 g wet cells were suspended in 160 ml of 10 mM sodium phosphate buffer (pH 7.0) supplemented with 3 mM PMSF (phenylmethanesulfonyl fluoride), and were broken by ultrasonication at 4 °C. The crude extract was centrifuged at 95,000 × *g* for 90 min. The supernatant was loaded onto a Q-Sepharose column (2.5 × 10 cm) pre-equilibrated with 10 mM sodium phosphate (pH 7.0). HMC passed through the column without binding, and then the passed fraction was applied to an SP-Sepharose column (2.5 × 10 cm). After washing with 3 column volumes of equilibration buffer, HMC fractions were eluted by a linear gradient of 0–200 mM NaCl in 10 mM Sodium phosphate buffer (pH 7.0). The HMC fractions were further purified by a Sephacryl S-200 (2.6 × 60 cm) gel filtration column chromatography.

2.2. Crystallization

The crystals were prepared using the hanging drop vapor diffusion method. 3 μl of the protein droplets containing 15 mg/ml HMC in 10 mM sodium phosphate buffer (pH 7.0) and 200 mM NaCl were equilibrated to 3 μl of reservoir solution containing 40% PEG600 in 0.1 M MES buffer (pH 5.7) (2-morpholinoethanesulfonic acid). The crystal for the diffraction study was grown from the protein sample in the oxidized states.

Table 1

Statistics of data collection.

Stages (state)	1 st stage (transient)	2 nd stage (reduced) [‡]			
Frames	1-45	1-180 (merged data)	1-60	61-120	121-180
No. of frames	45	180	60	60	60
Exposure time per frame (sec)	60	30	30	30	30
Total exposure (min) [†]	45	135	75	105	135
No. of observations	92,212	368,976	123,321	123,002	122,689
No. of unique reflections	15,910	16,963	16,423	16,962	16,939
Completeness* (%)	93.3 (93.3)	100 (100)	96.6 (96.6)	99.9 (99.9)	99.9 (99.9)
R_{merge}^*	0.067 (0.221)	0.093 (0.355)	0.083 (0.310)	0.084 (0.356)	0.079 (0.308)
I/σ *	8.7 (2.1)	6.9 (2.0)	7.2 (2.3)	7.1 (2.1)	7.6 (2.2)

[†]Accumulated exposure time at the end of the set from the first diffraction data set.

[‡]The data set of reduced state was divided into three sets of 60 frames (frame No 1-60, 61-120 and 121-180).

*The values in parentheses are for the highest resolution shell (2.80-2.95 Å).

2.3. X-ray diffraction data collection and processing

X-ray diffraction data sets were collected at the BL44B2 beam line in SPring-8, Japan using a MAR CCD system. The crystal was mounted on a cryo-loop and flash-frozen in a nitrogen stream at 90 K. The crystal-to-detector distance was 200 mm, and the wavelength of x-ray beam was set to 1.0 Å. In the first stage of data collection, data set consists of 45 frames was collected with 1° oscillation angle and an exposure time of 60 sec per frame. After an absorption spectrum was measured, three data sets of a total of 180 (1-60, 61,120, and 121-180) frames with 1° oscillation angle and exposure time of 30 sec per frame were collected in the second stage. The crystal belongs to a hexagonal space group $P6_2$ with unit cell dimensions $a=108.3$ Å, $c=102.7$ Å and $\gamma=120^\circ$. The crystal diffracted to 2.8 Å. The data sets were indexed using MOSFLM (Leslie, 1994), and merged into one data set by scaling using the program SCALA (Collaborative Computational Project, Number 4, 1994). The completeness of each data set was sufficiently high. Data collection statistics are listed in Table 1.

2.4. Microspectrophotometry

Before the x-ray data collection, an absorption spectrum of the crystal was measured at 90 K using the microspectrophotometer (Sakai *et al.*, 2002) equipped on the BL44B2 beam line. Immediately after a total of 45 min x-ray exposure for the first data set collection, another absorption spectrum was measured. The third measurement was performed after data collection in the second stage (total x-ray exposure time = 135 min).

The ratio of absorbance $A_{552\text{ nm}} / A_{523\text{ nm}}$ (= 1.8) in the reduced form of the sample solution in this study showed well coincidence with the value reported by Ogata *et al.* The corresponding values in the crystal of HMC after 45 min (Fig.1(c)) and 135 min (Fig.1(d)) exposure of x-ray are smaller than 1.8, indicating that the crystal even at 135 min x-ray exposure was not fully reduced. Absorbance of α peak is defined by:

$$A_{552\text{ nm}}(\text{obs}) = A_{552\text{ nm}}(\text{oxi}) + A_{552\text{ nm}}(\text{red})$$

where $A_{552\text{ nm}}(\text{oxi})$ and $A_{552\text{ nm}}(\text{red})$ are peak heights of the spectrum derived from oxidized and reduced hemes. This equation can be

converted using population of reduced heme x and absorption coefficient $\epsilon_{552\text{ nm}}(\text{oxi})$ and $\epsilon_{552\text{ nm}}(\text{red})$ as follows:

$$A_{552\text{ nm}}(\text{obs}) = (1-x)\epsilon_{552\text{ nm}}(\text{oxi}) + x\epsilon_{552\text{ nm}}(\text{red})$$

The similar equation is defined at 523 nm (β peak):

$$A_{523\text{ nm}}(\text{obs}) = (1-x)\epsilon_{523\text{ nm}}(\text{oxi}) + x\epsilon_{523\text{ nm}}(\text{red})$$

The ratio, $A_{552\text{ nm}}(\text{obs}) / A_{523\text{ nm}}(\text{obs})$ gives the following equation:

$$\frac{A_{552\text{ nm}}(\text{obs})}{A_{523\text{ nm}}(\text{obs})} = \frac{\{(1-x)\epsilon_{552\text{ nm}}(\text{oxi}) + x\epsilon_{552\text{ nm}}(\text{red})\}}{\{(1-x)\epsilon_{523\text{ nm}}(\text{oxi}) + x\epsilon_{523\text{ nm}}(\text{red})\}} \quad (1)$$

In this result, the population x was determined from the equation (1) by using experimental values of $A_{552\text{ nm}} / A_{523\text{ nm}}$ and the ϵ s.

2.5. Structure determination and refinement

Starting coordinates used for the structure analysis by a molecular replacement method were 2.8 Å structure of HMC from *Desulfovibrio vulgaris* Miyazaki (unpublished data). The initial HMC model for *D. v.* Hildenborough was obtained by using the first diffraction data set (Table 1). The structure refinement for each data set was performed using the program CNS (Brünger *et al.*, 1998). At the step of the simulated annealing at 2500K, atomic B-factors were individually refined. The molecular model was manually corrected and water molecules were picked up in the electron density map calculated after the several refinement steps. Since the microspectroscopic measurement revealed that the crystal was almost reduced (86%) after 45 min exposure of the x-ray beam in the first stage of the measurement (see section 3.2) and the crystal was no longer reduced during the following data collection, the three data sets (1-60, 61-120, and 121-180 frames in Table 2) collected in the second stage were merged into one data set. The final refinement statistics are shown in Table 2.

Table 2

Final refinement statistics.

Stages (state)	1 st stage (transient)	2 nd stage (reduced)			
Frames	1-45	1-180 (merged data)	1-60	61-120	121-180
Resolution limits (Å)		30-2.8			
R_{work} (%)	24.9	23.4	24.2	24.0	23.8
R_{free} (%)	33.5	29.7	29.4	29.9	31.0
No. of protein atoms	3,690	3,690	3,690	3,690	3,690
No. of heme atoms	688	688	688	688	688
No. of water molecules	47	51	45	36	38
Rms bond distances (Å)	0.0160	0.0161	0.0168	0.0169	0.0171
Rms bond angles (°)	4.950	4.944	4.853	4.847	4.898

^{*} $R = \sum_{\text{hkl}} | |F_{\text{obs}}| - k|F_{\text{calc}}| | / (\sum_{\text{hkl}} |F_{\text{obs}}|)^{1/2}$.

For the test set 5% of reflections were randomly chosen in the resolution range (Brünger, 1992).

3. Results and discussions

3.1. Purification and crystallization

The recombinant HMC was obtained from the *Shewanella oneidensis* expression system and purified by an ion-exchange and

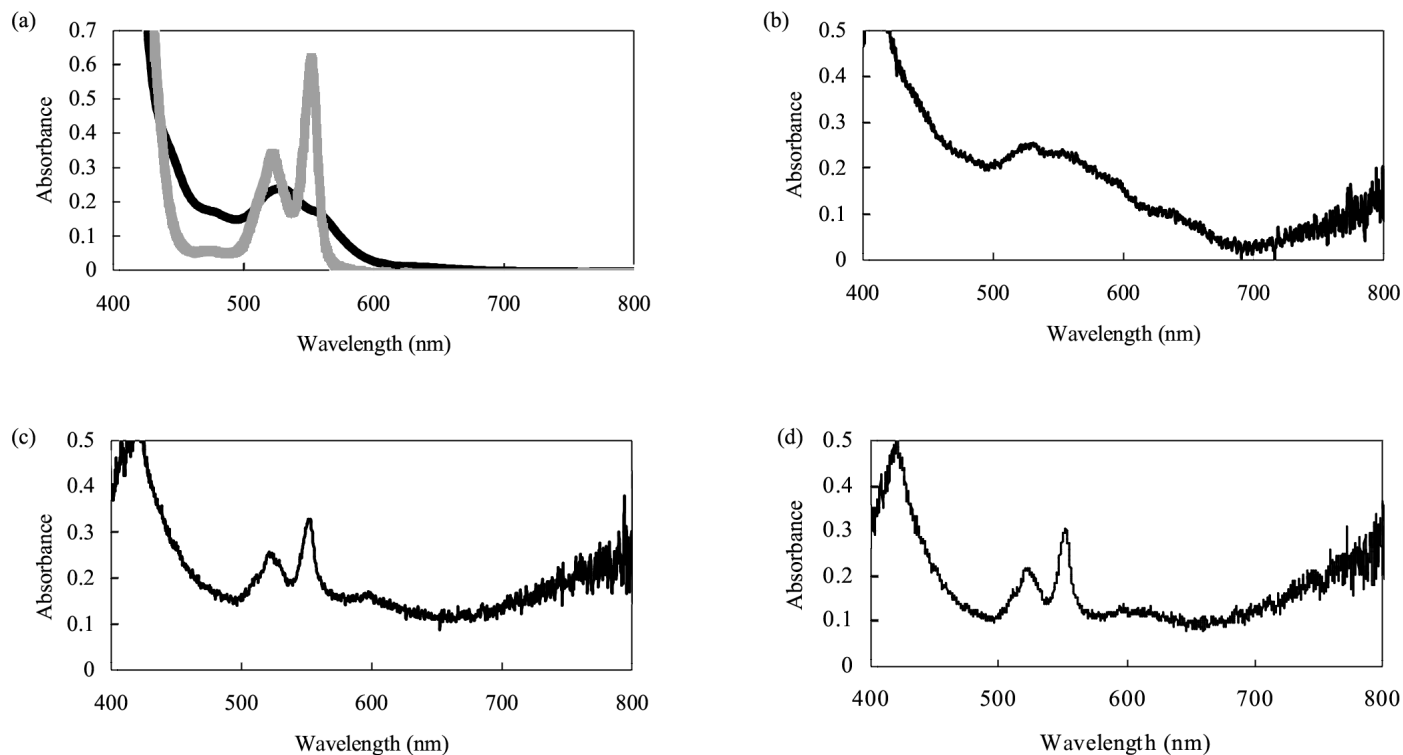


Figure 1

The absorption spectra of HMC from *D. vulgaris* Hildenborough (400–800 nm). The spectrum in the reduced state has two typical peaks at 552 and 523 nm in the range 400–800 nm. (a) Spectrum of the HMC in the oxidized (as-isolated, in black) and dithionite reduced (in grey) states in solution.

gel-filtration chromatography. The yield of the protein was estimated from the absorption spectrum as 6.1 mg from 16 g wet cells. Single crystals grew within one week to a typical size of $0.2 \times 0.05 \times 0.1 \text{ mm}^3$ in the oxidized (as-isolated) state. The absorption spectra of HMC in the oxidized and reduced states in solution are shown in Fig. 1(a).

3.2. Microspectroscopy

The spectrum before illumination of x-ray beam is shown in Fig. 1(b). The spectrum indicates that the crystal was in the oxidized state. The spectrum after 45 min x-ray exposure shows that the crystal was significantly reduced (Fig. 1(c)). Population of the reduced hemes in the crystal was estimated as 86% from the equation (1) by using the millimolar extinction coefficients at 523 and 552 nm obtained from the HMC solution in both the oxidized and reduced states.

Fig. 1(d) shows the absorption spectrum after 90 min exposure of x-ray beam for data collection in the second stage (total exposure time is 135 min from the starting time of the first diffraction data set). The peak ratio of this spectrum indicates that the reduced-heme content is about 95%. These results suggest that reduction of hemes no longer proceeded after 45 min exposure of x-ray beam. This might be caused by the trace of the oxidizing agent remained in the crystal. Based on these microspectroscopic measurements, we assigned the structure obtained from the first data set as the transient state from the oxidized to the reduced state, whereas those from the data sets in the second stage as the reduced state.

(b) Spectrum of the HMC crystal in the oxidized state before x-ray exposure.
(c) Spectrum of the HMC crystal after 45 min of x-ray exposure.
(d) Spectrum of the HMC crystal after 135 min of x-ray exposure.

3.3. Comparison of structures

Fig. 2 shows a stereo view of the folding pattern of HMC molecule determined from the first (transient) and second (reduced) data sets (note that three data sets in the second stage were merged). Both structures contain the residues from 40 to 545 and 16 heme groups except for some residues of 283–289, 392–395, and 500–506, which could not be assigned in the electron density map. It should be noted that both R_{work} and R_{free} of the transient structure are higher than those of the reduced structure. This might indicate that the diffraction intensities were changed by the transition of the molecular structure, which is concerted with the reduction of heme groups by x-ray exposure.

This is consistent with the results that the overall RMSD between the structures of the transient and the reduced states (0.65 Å) is slightly larger than the values (0.55–0.59 Å) calculated between three data sets of the second diffraction experiment for the reduced structure.

Though the resolution of the present structures are not high enough to discuss coordination geometry of the hemes in detail, it is worth to mention Fe–Nε2 (His) bond lengths: the distances between Fe of heme and Nε2 of His residue range 1.92–2.07 Å and 1.94–2.11 Å for the transient and reduced states, respectively. This result is not surprising because no large differences of Fe–Nε2 (His) distance, in fact, have been found between the oxidized and reduced states in the published papers on atomic structures of cytochromes (Norager *et al.*, 1999).

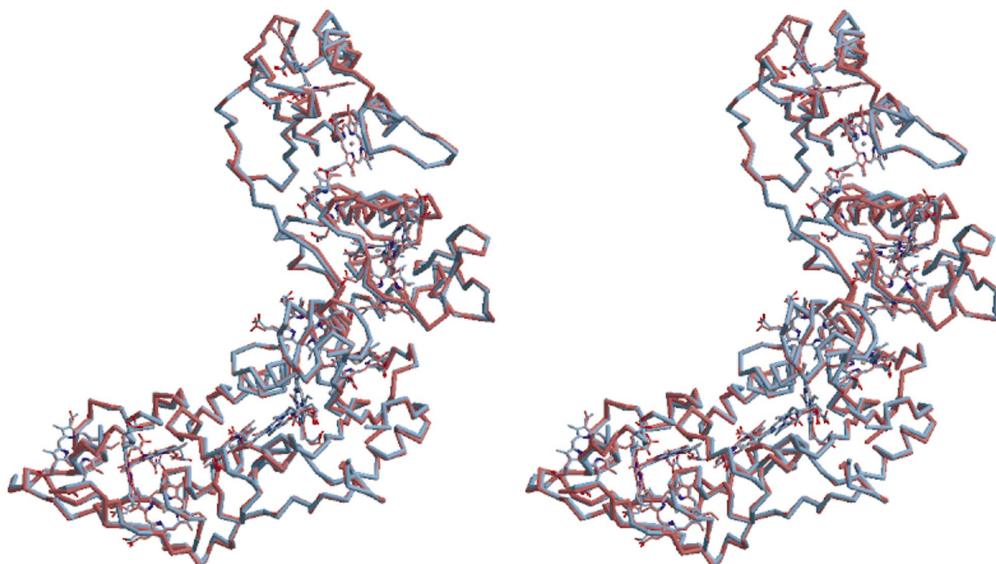


Figure 2

The comparison of the main-chain folding of HMC between the transient (red) and reduced (blue) states. The figure was generated using MOLSCRIPT (Kraulis, 1991) and Raster3D (Merrit and Murphy, 1994)

4. Concluding remarks

Synchrotron source has enabled us to collect diffraction data even for very small crystals, which are usually difficult to obtain complete data set with an in-house generator. It often brings, however, substantial radiation damage derived from hydrated electrons, hydroxyl and hydrogen radicals (Burmeister, 2000), and heat generation. Radiation damage itself can be now reduced by the recent development of the cryogenic technique to freeze radical species and crystals during data collection. It is, however, concluded by the present microspectrophotometric analysis of the irradiated crystal that the conventional cryogenic technique is not sufficient to keep the heme proteins in crystalline state as it is in the oxidized state during x-ray exposure. The results presented here suggest that the structures of the heme proteins solved using the brilliant x-ray beam may contain the transient states from the oxidized to reduced states.

We thank Dr. S. Adachi in RIKEN for his assistance with microspectroscopy measurements and Dr. K. Suto in NIAS for her valuable advice. This work was supported in part by grants from 21st Century COE Program, and National Project on Protein Structural and Functional Analyses to YH.

References

Brünger, A.T. (1992). *Nature* **335**, 472-474.
 Brünger, A.T., Adams, P.D., Clore, G.M., DeLano, W.L., Gros P., Grossbard, R.J., Rice, L.M., Simonson, T. and Warren, G.L. (1998). *Acta Cryst. D* **54**, 905-921.
 Burmeister, W.P. (2000). *Acta Cryst. D* **56**, 328-341.
 Collaborative Computational Project, Number 4 (1994). *Acta Cryst. D* **50**, 760-763.
 Czjzek, M., Payan, F., Guerlesquin, F., Bruschi, M., Haser, R. (1994). *J. Mol. Biol.* **243**, 653-67.
 Czjzek, M., Guerlesquin, F., Bruschi, M. and Haser, R. (1996). *Structure* **4**, 395-404.

Czjzek, M., Arnoux, P., Haser, R. and Shepard, W. (2001). *Acta Cryst. D* **57**, 670-678.
 Czjzek, M., ElAntak, L., Zamboni, V., Morelli, X., Dolla, A., Guerlesquin, F. and Bruschi, M. (2002). *Structure* **10**, 1677-1686
 Fritz, G., Griesshaber, D., Seth, O. and Kroneck, P. M. (2001). *Biochemistry* **40**, 1317-1324.
 Haser, R., Pierrot, M., Frey, M., Payan, F., Astier, J. P., Bruschi, M., Le Gall, J. (1979). *Nature* **282**, 806-10.
 Higuchi, Y., Kusunoki, M., Matsuura, Y., Yasuoka, N. and Kakudo, M. (1984). *J. Mol. Biol.* **172**, 109-139.
 Higuchi, Y., Inaka, K., Yasuoka, N. and Yagi, T. (1987). *Biochim. Biophys. Acta*, **243**, 214-224
 Higuchi, Y., Yagi, T. and Yasuoka, N. (1997). *Structure*, **5**, 1671-1680
 Ishimoto, M., Koyama, J. and Nagai, Y. (1954). *Bull. Chem. Soc. Japan* **27** 564-565.
 Kraulis, P.J. (1991). *J. Appl. Cryst.* **24**, 946-950.
 Laskowski, R.A., MacArthur, M.W., Moss, D.S. and Thornton, J.M. (1993). *J. Appl. Cryst.* **26**, 283-291.
 Leslie, A.G.W. (1994). MOSFLM version 5.41 MRC laboratory of Molecular Biology, Cambridge, UK.
 Matias, P. M., Saraiva, L. M., Soares, C. M., Coelho, A. V., LeGall, J. and Carrondo, M. A. (1999). *J. Biol. Inorg. Chem.* **4**, 478-494.
 Matias, P. M., Morais, J., Coelho, R., Carrondo, M. A., Wilson, K., Dauter, Z., Sieker, L. (1996). *Protein Sci.* **5**, 1342-54.
 Matias, P. M., Coelho, A. V., Valente, F. M., Placido, D., LeGall, J., Xavier, A. V., Pereira, I. A. and Carrondo, M. A. (2002). *J. Biol. Chem.* **277**, 47907-47916
 Merrit, E.A. and Murphy, M.E. (1994). *Acta Cryst. D* **50**, 869-873.
 Morimoto, Y., Tani, T., Okumura, H., Higuchi, Y. and Yasuoka, N. (1991). *J. Biochem (Tokyo)*. **110**, 532-540.
 Nakagawa, A., Higuchi, Y., Yasuoka, N., Katsube, Y. and Yagi, T. (1990). *J. Biochem (Tokyo)*. **108**, 701-703.
 Norager, S., Legrand, P., Pieulle, L., Hatchikian, C. and Roth, M. (1999). *J. Mol. Biol.* **290**, 881-902.
 Ogata, M., Kiuchi, N., Yagi, T. (1993) *Biochimie*. **75**, 977-983.
 Ozawa, K., Yasukawa, F., Fujiwara, Y. and Akutsu, H. (2001). *Biosci. Biotechnol. Biochem.* **65**, 185-189.
 Pierrot, M., Haser, R., Frey, M., Payan, F., Astier, J. P. (1982). *J. Biol. Chem.* **257**, 14341-8.
 Pollock, W. B., Loutfi, M., Bruschi, M., Rapp-Giles, B. J., Wall, J. D. and Voordouw, G. (1991). *J. Bacteriol.* **173**, 220-228.
 Ravelli, R.B.G., Leiros, H.-K.S., Pan, B., Caffrey, M., and McSweeney, S. (2003). *Structure* **11**, 217-224.
 Ramachandran, S. (1968). *Adv. Prot. Chem.* **23**, 283-437.
 Rossi, M., Pollock, W. B., Reij, M. W., Keon, R. G., Fu, R. and Voordouw, G. (1993). *J. Bacteriol.* **175**, 4699-4711.
 Sakai, K., Matsui, Y., Kouyama, T., Shiro, Y. and Adachi, S. (2002). *J. Appl. Cryst.* **35**, 270-273.
 Yagi, T. (1969) *J. Biochem. (Tokyo)* **66**, 473-478.